Properties of Si:H Mixed Amorphous Microcrystalline Phases

C. R. Wronski and R. W. Collins

Center for Thin Film Devices, the Pennsylvania State University, University Park, PA 16802

Introduction

Researchers at The Pennsylvania State University have shown that the thin film Si:H prepared under moderate-to-high H_2-dilution conditions with low temperature rf plasma enhanced chemical vapor deposition (PECVD) evolves from the amorphous phase to a mixed amorphous + microcrystalline phase [(a+μc)-Si:H] with the accumulated thickness of the layer. The thin film material in the amorphous regime of growth has been called "*protocrystalline*" Si:H and exhibits a higher degree of ordering than materials deposited under similar conditions without H_2-dilution [1-3]. Furthermore they showed that the phase evolution of this material with thickness and, in particular, the transition to the mixed-phase (a+μc)-Si:H material, depends not only on hydrogen dilution ratios, $R=[H_2]/[SiH_4]$, but also on the substrate material. Consequently, without using real time spectroscopic ellipsometry (RTSE) or equally powerful techniques, it is not possible to control the growth of the protocrystalline Si:H materials and cell structures or to characterize their properties reliably. The insights into the growth process and microstructural evolution into the (a+μc) mixed Si:H phase obtained from RTSE have been extended to characterization of the optoelectronic properties of these phase and their effect on solar cell properties.

Growth and Microstructural Evolution of Protocrystalline Si:H

A key capability of RTSE is the ability to generate deposition phase diagrams for different R, different deposition conditions and different substrate materials. In such a diagram, the transition thicknesses are plotted as continuous functions of a key deposition parameter. In low temperature PECVD, R is used as the abscissa of the phase diagram since it exerts the greatest control over the phase of the film -- from a-Si:H at low R to μc-Si:H at high R. Over a wide range in R, however, Si microcrystallites have been observed to nucleate from within the growing a-Si:H phase after a critical phase-transition thickness that decreases with increasing R.

The phase diagrams have led to the concept of *protocrystalline* Si:H deposition. There are three important characteristics of this film growth regime. As its name implies, the protocrystalline growth regime is one in which a-Si:H is deposited initially, but given sufficient accumulated thickness, microcrystallites nucleate from the amorphous phase. Thus, the growing film will ultimately evolve first to mixed-phase (a+μc)-Si:H and finally to single-phase μc-Si:H. Once the a→(a+μc) transition is detected, however, the growing material is no longer considered protocrystalline. A second characteristic of the protocrystalline growth regime is the substrate dependence of the phase of the growing material. If the Si:H film grows in the protocrystalline regime on a freshly-deposited amorphous film substrate (such as R=0 a-Si:H), the same deposition conditions would lead to single-phase microcrystalline silicon growth on a freshly-

deposited μc-Si:H substrate film. Thus, under protocrystalline growth conditions, local epitaxy is favored on a c-Si substrate; however, crystallite nucleation is suppressed on an amorphous substrate. A third characteristic of the protocrystalline growth regime is the observed enhanced degree of nuclei coalescence that yields the smoothest surfaces among a-Si:H films on an amorphous substrate.

At moderate to high values of R, however, a roughening transition is observed in which crystallites nucleate from the growing amorphous phase. Because the nucleation density is usually low and the crystallites grow preferentially, the crystalline protrusions generate a surface roughness layer that increases rapidly in thickness with the bulk thickness, d_b. Once the growing film crosses this transition and the crystallite volume fraction exceeds a critical value, the (a+μc) mixed phase material becomes unsuitable as an i-layer component of an a-Si:H-based solar cell. For thin films that have already undergone the a→(a+μc) transition, a second transition is possible that occurs at even greater bulk layer thickness. In this transition, the crystalline protrusions that extend above the surface have become large enough to make contact, leading to a crystallite coalescence process with continued film growth. This process is manifested in the data as a transition from surface roughening to smoothening during mixed-phase film growth. Once the crystallites have coalesced to cover the growing film surface completely, single-phase μc-Si:H growth proceeds with a resumption of surface roughening. For optimum μc-Si:H i-layers in solar cells, one generally seeks to deposit the film using the lowest R value possible while maintaining the film within the microcrystalline growth regime throughout the deposition. The evolution of the roughness layer thickness, d_s, as a function of bulk layer thickness, d_b, for three values of R are shown in Figure 1.

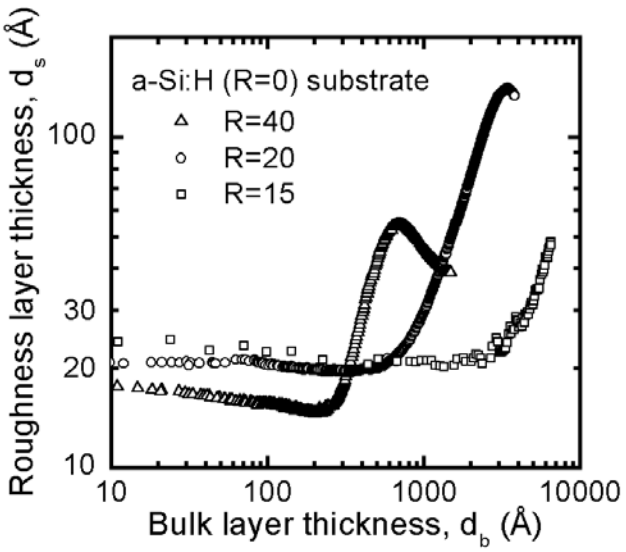

Figure 1. Surface roughness layer thickness (d_s) versus bulk layer thickness (d_b) extracted in analyses of RTSE data collected during the deposition of Si:H with R=15, 20, and 40, all on R=0 a-Si:H substrate films.

The a→(a+μc) roughening transitions, and the (a+μc)→μc smoothening transitions can be incorporated readily into deposition phase diagrams. The phase diagram depends not only on the other fixed deposition conditions, such as R, plasma power, substrate temperature, and total gas pressure, but also on the substrate since the latter exerts a strong influence over crystallite nucleation. Deposition phase diagrams are very convenient in the design of devices since they describe the regimes of layer thickness and deposition parameter space within which single-phase a-Si:H, (a+μc)-Si:H, and single-phase μc-Si:H are obtained [4]. As a review of such phase diagrams, Figure 2 is presented which shows the proposed schematic structure of ~5000 Å thick Si:H films on R=0 a-Si:H substrate films, given as a continuous function of R along with the thicknesses of the a→(a+μc) and (a+μc)→μc transition boundaries. There are several important features illustrated in Fig. 2 that should be pointed out. The first is

the continuous decrease with R of the thickness at which the transition of protocrystalline a-Si:H into the a+μc phase occurs. This characteristic has very important consequences in the design of protocrystalline solar cells with different thickness which until now have not been recognized [5]. Another feature is the increase with R in the nucleation density of μc-Si at the a→a+μc transition which are key to the subsequent growth of the a+μc mixed phase. A third point that can be made is the decrease with R of the range of boundaries between which the a+μc Si:H phase present before coalescing into the μc Si:H phase.

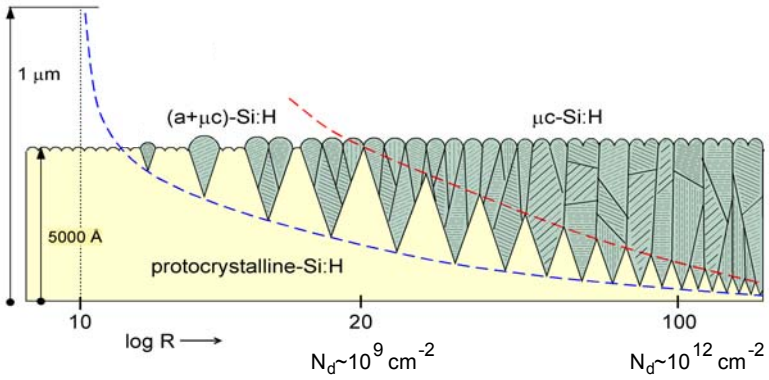

Figure 2. Schematic of the structure of Si:H films prepared as a function of R. The dashed and dotted lines identify the a→(a+μc), and (a+μc)→μc transitions, respectively. Also indicated are the corresponding densities of μc-Si:H nuclei present at the a→(a+μc) transition.

Correlations of the phase diagrams for intrinsic Si:H layers with the corresponding electronic properties and p-i-n device performance demonstrate that the optimum i-layers for a-Si:H p-i-n and n-i-p solar cells are obtained at the maximum possible R value for the desired thickness without crossing the a→(a+μc) boundary of the phase diagram into the mixed-phase growth regime [6]. It should be emphasized that because the R value at this phase boundary depends on both the nature of the substrate and the i-layer thickness, these aspects of the materials or device structure must be specified in order to identify the optimum conditions. The unique characteristic of protocrystalline Si:H is that not only is it a superior optoelectronic material but also its higher stability to light induced degradation as measured for both materials and devices.

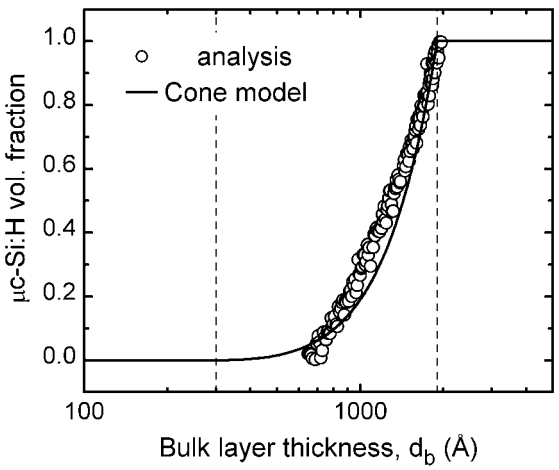

Figure 3. Depth profile in the volume fraction of the microcrystalline phase throughout the mixed-phase (a+μc) Si:H growth regime for the R=20 Si:H deposition on c-Si from Fig. 1 (points). Also shown as the solid line is the prediction of the microcrystallite cone growth model depicted in Figure 4.

In order to extract the thickness evolution of the μc-Si:H volume fraction in mixed (a+μc) Si:H i-layers, a new method of RTSE analysis had to be developed. In the analysis, the thickness at which crystallites first nucleate from the a-Si:H phase can be estimated, as well as the nucleation density and microcrystallite growth [7, 8]. Figure 3 shows the evolution of the volume fraction of μc-Si:H in a R=20 film throughout the growth regime starting from the a→(a+μc) transition and ending near the (a+μc)→μc transition. These results are modeled as a mixture of a-Si:H and μc-Si:H of variable volume fractions $1-f_{\mu c}$ and $f_{\mu c}$,

respectively, and a surface roughness layer, modeled as a mixture of the outerlayer material and void with fixed volume fractions of $1-f_{sv}$ and f_{sv}, respectively. The solid line in Fig.3 is the result for $f_{\mu c}$ versus $d_{b,}$ the thickness of the film, established using the cone model of microcrystallite evolution. Figure 4 identifies how this microcrystallite cone model is constructed. In this model, it is assumed that all microcrystalline nuclei originate at the a→(a+μc) transition layer thickness ($d_{b,trans}$). The area density of such nuclei is assumed to be N_d, and the nuclei are assumed to grow preferentially at the expense of the surrounding a-Si:H phase with a constant, thickness-independent cone angle, θ. For example, for the deposition of Fig. 3, values of θ=19° and N_d=1.1x10^{10} cm^{-2} are determined.

Figure 4 presents results for the cone angle θ and the nucleation density N_d plotted as a function of the a→(a+μc) transition thickness for a series of Si:H films prepared on both c-Si and R=0 a-Si:H substrates under different conditions of H_2-dilution, plasma power, and substrate temperature. Results deduced solely from RTSE using this approach have been compared and found to be completely consistent with those from cross-sectional transmission electron microscopy (XTEM) and from atomic force microscopy (AFM). It is found that the nucleation density decreases significantly with increasing a→(a+μc) transition thickness, yet the crystallite cone angle is nearly constant between 15° and 20°. The consistency between the indirect (but real time) optical measurements and the direct (but ex situ) structural measurements, providestrong support for the generality of the cone growth model for microcrystallinity as depicted in Fig. 4.

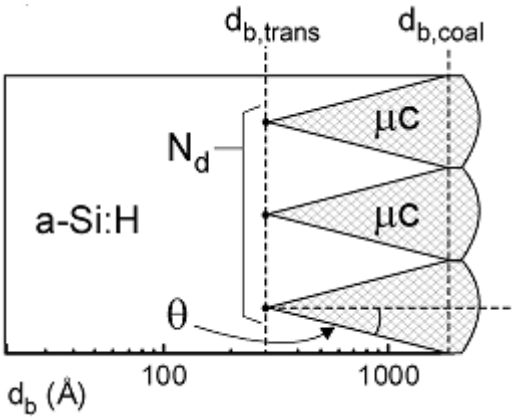

Figure 4. Schematic of the cone growth model used to estimate the microcrystallite nuclei density and cone angle.

Optoelectronic and Solar Cell Properties of Mixed Amorphous Microcrystalline Phases

The systematic studies employing RTSE have described the transitions from the amorphous protocrystalline to the microcrystalline phase as well as the microstructure of the (a+μc) phase as a function of the accumulated thickness for Si:H films prepared at moderate-to-high R (10≤R≤100). These studies suggest that the electronic transport properties in such materials are anisotropic as well as thickness-dependent, and as a result, it is problematic to characterize the electrical properties of the films assuming homogeneity versus thickness. Furthermore, difficulties are encountered when attempting to correlate basic material and device properties because of the differences in transport behavior arising from the inhomogeneity and anisotropy.

Detailed studies have been carried out on the optoelectronic and solar cell properties of protocrystalline Si:H which have been characterized in detail [6]. The optoelectronic and solar cell properties of the mixed-phase (a+μc)-Si:H and single phase μc-Si:H layers have been investigated by incorporating them into the i-layers of p-i-n solar cell structures and interpreting their effects on device characteristics. The experimental approach was to assess the effects of these layers by comparing results for cell structures absent any a→μc transition layers with those

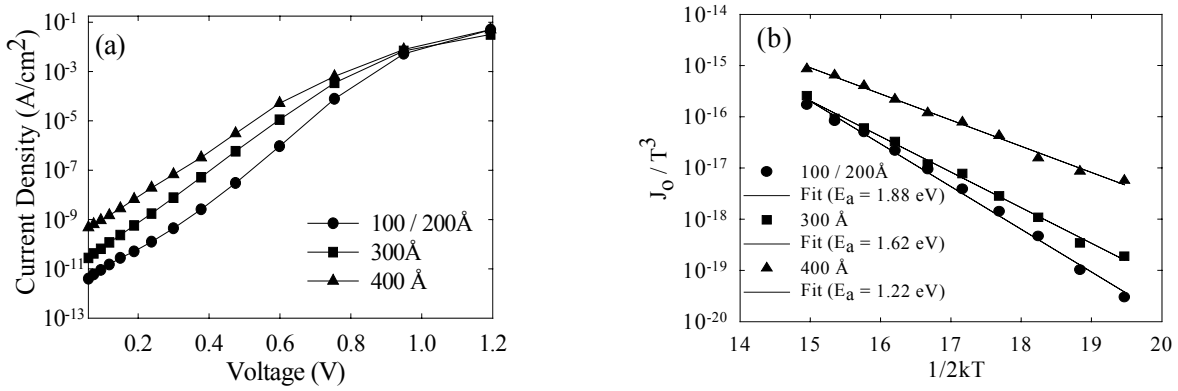

Figure 5. (a) Experimental dark J-V characteristics of 4000Å p-i-n cells having R=10 bulk i-layers and different thickness R=40 p/i interface layers. (b) Thermal activation plots of J_o/T^3 for the cells shown in (a). The symbols are experimental results and the solid lines are exponential fits used to extract E_μ.

for structures incorporating such layers at different depths from the p/i interface. In such studies, information about the depth profile of the i-layer mobility gaps was obtained from the solar cell light and dark J-V characteristics and their temperature dependence, as well as from numerical modeling of these characteristics [9, 10].

It was found that for optimized p-i-n a-Si:H solar cells having high quality contact and interface regions, the dark currents at low forward bias voltages are determined by recombination rates in the bulk i-layer which are exponentially dependent on its mobility gap (E_μ) [10]. The E_μ value of the i-layer plays a key role in transport and collection of photo-generated carriers under illumination and in cells whose characteristics are dominated by the properties of the bulk i-layer [11]. With homogeneous i-layers the dark J-V characteristics exhibit the classical exponential diode behavior wherein J_o can be obtained from the intercepts of the linear regions of the semi-log plots. It was found that reliable E_μ values can be obtained from the dependence of J_o on temperature in such p-i-n cells when interface recombination is sufficiently low so that J_o is primarily determined by recombination-generation in the bulk i-layer. The dependences of J_o/T^3 on temperature then yield well-defined slopes with values of E_μ that are in excellent agreement with the values measured with internal photoemission [12].

The correlations among carrier recombination kinetics in the bulk i-layer, J_o, and E_μ established for p-i-n cells with homogeneous i-layers were then extended to include the more complicated cases of cells with evolving i-layers such as described here. This included a study carried out on a series of R=10 protocrystalline p-i-n cells each with a total i-layer thickness of 4000 Å, where a R=40 layer was incorporated at the p/i interface of each cell with the thicknesses ranging from 100 Å to 400 Å. Insights into the electronic properties of the transition material from amorphous to mixed-phase Si:H and then to single-phase μc-Si:H that give rise to deleterious effects on cell performance could be obtained from the dark J-V characteristics of the cells as shown in Fig. 5a. The increase in carrier recombination-generation (R-G) in the vicinity of the phase transition region can be directly inferred from the systematic increase of the dark currents in the exponential region as the R=40 Si:H layer thickness increases from 100 to 400 Å and traverses the phase boundary as indicated in Fig. 2. The increase by two orders of magnitude in the room temperature value of J_o clearly indicates a large increase in R-G currents

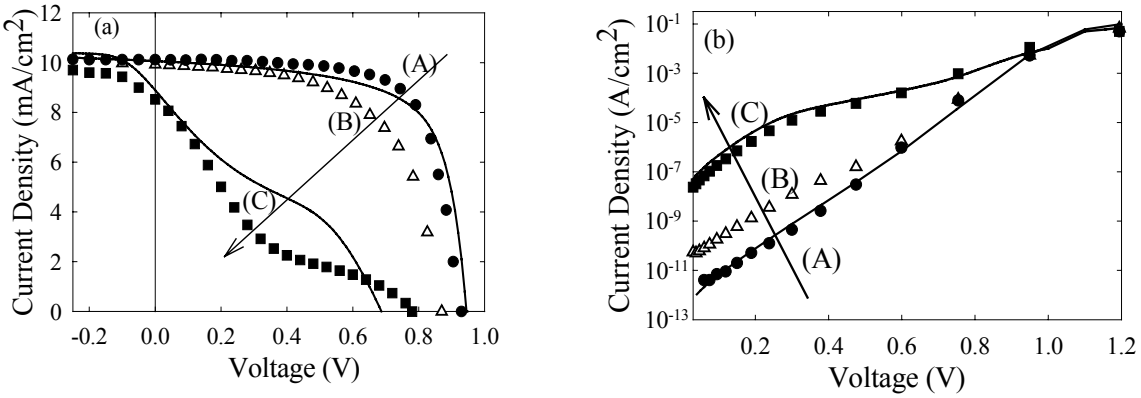

Figure 6. Experimental data (symbols) and simulations (solid lines) for the J-V characteristics of cells A, B, and C measured at room temperature (a) under 1 sun illumination and (b) in the dark. Direction of the arrows indicate decreasing distance between the a→(a+μc) transition and p-contact.

that can be attributed primarily to changes in the mobility gap. This is evident from Fig. 5b wherein plots of J_o/T^3 versus $(2kT)^{-1}$ are shown for the results in Fig. 5a. The decreases of E_μ to 1.66 eV for the 300 Å interface layer and to 1.22 eV for the 400 Å layer indicate that over a thickness of 200 Å there is a transition from the amorphous phase to a material having a mobility very close to that of bulk microcrystalline Si:H.

Additional insights into the transitions as well as their effect on cell characteristics of 4000 Å thick cell structures could be obtained from a study carried out on a cell in which a 400 Å R=40 p/i interface (similar to that described above) was followed by an R=20 bulk i-layer region (referred to here as cell C). The characteristics of this cell were then compared with those of the optimized structure described above having a 200 Å R=40 p/i interface and a homogeneous R=10 bulk region (referred to as cell A), as well as a cell deposited with a one-step R=20 i-layer (referred to as cell B). Ellipsometry studies show that the a→(a+μc) transition in the R=20 layer deposited on an amorphous film occurs after an accumulated film thickness of approximately 1000 Å, while on a R=40 layer that has traversed the phase boundary it proceeds in the microcrystalline phase so that the i-layer is fully microcrystalline. The experimental J-V results at room temperature for cells A, B, and C are shown in Figs. 6a and 6b under 1 sun illumination and in the dark, respectively. It can be seen in Fig. 6a that the FF and V_{oc} are the highest for cell A since the thickness and R values in the two step i-layer are chosen so that protocrystallinity is maintained. The cell performance becomes progressively worse for cells B and C as the position of the transition to mixed phase in the i-layer approaches the p-contact (indicated by the direction of the arrows).

This drop in cell performance is attributed to narrow gap material in the i-layer of cells B and C whose presence is reflected in the dark J-V characteristics as shown in Fig. 6b. The carrier recombination rates in a p-i-n cell can be explained by the large contribution of the narrow gap material to the recombination currents at low forward bias and the inflection points in the dark J-V characteristics observed in Fig. 6b. The simulation result shown in Fig. 6b (solid line) was carried out for cell C assuming a 400 Å wide gap Si:H layer with the remainder of the i-layer as a narrow gap μc-Si:H material having a mobility gap of 1.15 eV. The latter value was obtained

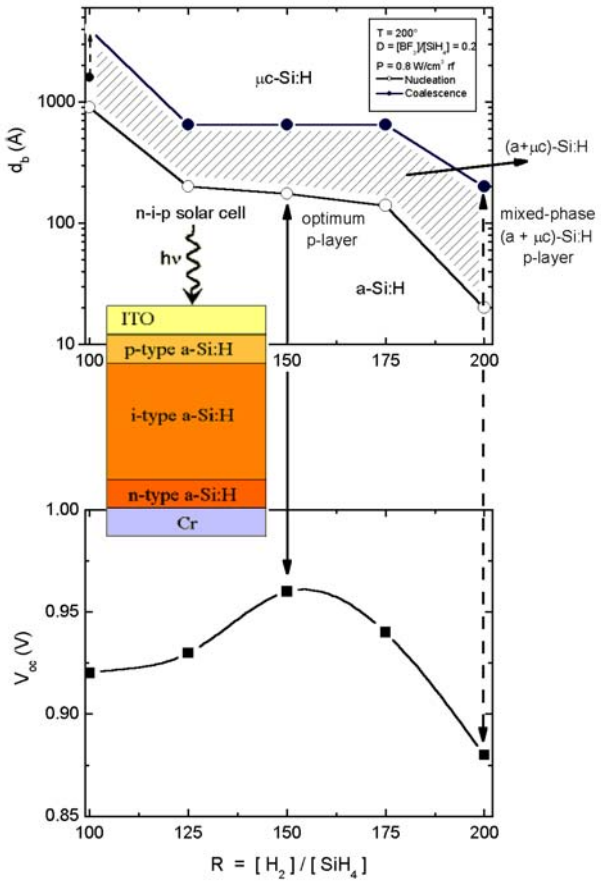

Figure 7. The extended phase diagram depicting the bulk thickness (Å) as a function of R for p-type Si:H deposition with BF_3 doping D=0.2 on a-Si:H substrates; also shown is 1 sun V_{OC} as function of R for solar cells with the corresponding 200Å p-layers.

experimentally from plot of J_o/T^3 vs. $(2kT)^{-1}$ for cell C. Both results suggest that the transition from the amorphous phase to a fully coalesced microcrystalline phase in the R=40 film occurs over a thickness of only a few hundred angstroms. The large decreases of the FF in cells B and C are a direct consequence of the phase transitions. Such characteristics could only be modeled for i-layers consisting of two distinctly different layers—a wide gap amorphous layer and a narrow gap microcrystalline one [13]. The results of the simulation for cell C is shown as a solid line in Fig. 6a, where the less than perfect fit is probably due to the necessary oversimplification of the highly anisotropic microcrystalline material when a one-dimensional simulator such as AMPS is being used.

The concept of protocrystallinity and the changes in E_μ present in the (a+μc) mixed Si:H phase was also successful in explaining the nature of p-type Si:H films doped with BF_3. Guided by the phase diagrams developed as function of R and doping concentrations it was possible to carry out a systematic development of high V_{OC} in n-i-p a-Si:H solar cells, such as illustrated in Figure 7 [14, 15]. The RTSE results, confirmed by TEM and AFM measurements, show that the optimum p-layers for obtaining high V_{OC} clearly lie within the protocrystalline amorphous Si:H growth regime without crossing into the mixed (a+μc) phase. It is interesting to note here that for a long time it has been proposed that highly doped μc Si:H layers have been responsible for obtaining high V_{OC}. This is due to the erroneous conclusions drawn about the thin p-layers in cells from results obtained on much thicker films in which the (a+μc) mixed and μc phases were present.

Summary

A brief review was presented of the growth and microstructure of *protocrystalline* Si:H, deposited by low temperature PECVD. This material cannot be adequately described as "edge material" as is often done because of the thickness dependence of the phase transition. The development of deposition phase diagrams from RTSE measurements was presented which identify the transition from amorphous → amorphous + microcrystalline to fully microcrystalline Si:H phases as function of different deposition parameters. Results were also presented on the

evolution of the microstructure in the (a+μc) Si:H mixed phase with thickness from the onset at the a → (a+μc) phase to its transition to a fully μc phase. Examples were then presented how RTSE was utilized in a *unique* approach for characterizing the optoelectronic properties of the (a+μc) mixed phase with highly anisotropic properties. Results were presented on p-i-n solar cells with controlled micro-structural composition in which the mobility gaps of the Si:H mixed amorphous microcrystalline phases were obtained. Meaningful correlations could be made between the materials and solar cell characteristics since in these studies the uncertainties associated with the initial nucleation and subsequent growth of Si:H films on different substrate materials were eliminated. The insights provided here into the transition from protocrystalline Si:H to mixed-phase Si:H and then to single-phase μc-Si:H are of critical importance to the engineering of cell structures with high performance and improved stability.

References:

1. R.W. Collins, A.S. Ferlauto, G.M. Ferreira, C. Chen, J. Koh, R.J. Koval, Y. Lee, J.M. Pearce and C. R. Wronski, *Solar Energy Materials and Solar Cells*, **78**, 143 (2003).
2. Y. Lu, S. Kim, M. Gunes, Y. Lee, C.R. Wronski, and R.W. Collins, *Mater. Res. Soc. Symp. Proc*. **336**, 595 (1994).
3. J. Koh, A.S. Ferlauto, P.I. Rovira, C.R. Wronski, and R.W. Collins, *Appl. Phys. Lett*. **75**, 2286 (1999).
4. J. Koh, Y. Lee, H. Fujiwara, C.R. Wronski, and R.W. Collins, *Appl. Phys. Lett*. **73**, 1526 (1998).
5. R.J. Koval, J. Koh, Z. Lu, L. Jiao, C.R. Wronski, and R.W. Collins, *Appl. Phys. Lett*. **75**, 1553 (1999).
6. C.R. Wronski, R.W. Collins, J.M. Pearce, R.J. Koval, X. Niu, A.S. Ferlauto, and J. Koh, *Mater. Res. Soc. Symp. Proc*. **715**, A.13-4.1 (2002).
7. R.W. Collins, A.S. Ferlauto, G. M. Ferriera, C. Chen, R.J. Koval, J.M. Pearce, and C.R. Wronski, *Mater. Res. Soc. Symp. Proc*. **762**, A5.10.1 (2003).
8. H. Fujiwara, Y. Toyoshima, M. Kondo, and A. Matsuda, *Phys. Rev. B* **60**, 13598 (1999).
9. R.J. Koval, J.M. Pearce, A.S. Ferlauto, R.W. Collins, and C.R. Wronski, *Mater. Res. Soc. Symp. Proc*. **664**, A16.4 (2001).
10. R.J. Koval, A.S. Ferlauto, J.M. Pearce, R.W. Collins, and C.R. Wronski, *J. Non. Cryst. Solids*, **299-302**, 1136 (2002).
11. J. Deng, J.M. Pearce, R.J. Koval, V. Vlahos, R.W. Collins, and C.R. Wronski, *Appl. Phys. Lett*. **82**, 3023 (2003).
12. C.R. Wronski, S. Lee, M. Hicks, and S. Kumar, *Phys. Rev. Lett*. **63**, 1420 (1989).
13. R.J. Koval, "Microstructurally Engineered Improvements in he Performance and Stability of Si:H Based Thin Film Solar Cells", PhD Thesis, The Pennsylvania State University, 2001.
14. R.J. Koval, C. Chen, GM. Ferreira, A.S. Ferlauto, J.M. Pearce, P.I. Rovira, C.R. Wronski, and R.W. Collins, *Appl. Phys. Lett*. **81**, 1258 (2002).
15. V. Vlahos, J. Deng, J.M. Pearce, R.J. Koval, R.W. Collins and C.R. Wronski, *Mat. Res. Soc. Proc*. **762**, A7.2 (2003).